atomes oxygène chacun à des distances moyennes de 2,057 et 2,045 Å respectivement.

Le Tableau 6 donne les valeurs de toutes les distances interatomiques dans les environnements des atomes de cuivre.

L'anion $PO_4^{3-}$ se présente comme un tétraèdre non régulier. La moyenne des distances P–O vaut 1,538 Å; elle est voisine de celle que l'on observe habituellement dans les phosphates (1,534 Å).

Les oxygènes isolés O(5) sont environnés de quatre ions cuivriques formant un tétraèdre presque régulier. Les seconds voisins de O(5) sont huit oxygènes à des distances comprises entre 2,61 et 3,03 Å. Le Tableau 7 indique les valeurs des distances interatomiques dans les tétraèdres $PO_4$ et dans l'environnement de l'oxygène isolé.

**Références**


BALL, M. C. (1968). *J. Chem. Soc.* (*A*), pp. 1113–1115.

BAUER, H. & BALZ, W. (1965). *Z. anorg. allgem. Chem.* **340**, 225–231.

BRIXNER, L. H. & FORIS, C. M. (1973). *J. Solid State Chem.* **7**, 149–154.

BROWN, J. J. & HUMMEL, F. A. (1964). *J. Electrochem. Soc.* **111**, 1052–1057.

BROWN, W. E. & EPSTEIN, E. F. (1965). *J. Res. Natl. Bur. Stand.* **69A**, 547–551.

PREWITT, C. T. (1966). *SFLS*-5. Report ORNL-TM-305. Oak Ridge National Laboratory, Tennessee.

SOKOLOV, V. A., RUBINCHIK, S. M., VANASHEK, E. I. & BUROVAYA, E. E. (1966). *Izv. Akad. Nauk SSSR, Neorg Mater.* **2**, 717–720. Traduction anglaise, pp. 616–618.


*Acta Cryst.* (1977). B**33**, 3468–3475

# The Structure of α-(AlFeSi) by Anomalous-Dispersion Methods


BY R. N. CORBY* AND P. J. BLACK†

*Department of Physics, The University of Birmingham, Birmingham* 15, *England*


(*Received* 21 *December* 1976; *accepted* 2 *May* 1977)


The compound α-(AlFeSi) has a hexagonal unit cell, $a = 12{\cdot}404 \pm 0{\cdot}001$, $c = 26{\cdot}234 \pm 0{\cdot}002$ Å, with 44·9 Fe, 167·8 Al and 23·9 Si atoms. 1800 diffraction spots were recorded photographically and measured at each of the Mo $K\alpha$, Fe $K\alpha$ and Co $K\alpha$ wavelengths by an automatic scanning technique. These data were analysed to give geometrical structure factors for the Fe atoms alone. The structural arrangement of the Fe atoms was obtained with a sign-determining method, and the result combined with the multiple-wavelength data to determine the whole structure. The final refinement with a full-matrix least-squares method gave an $R$ value of 5·7% for $F$ with the Mo $K\alpha$ data. The structure is described in terms of the linkage of the polyhedra of Al atoms which surround each Fe atom and is characterized by shortened Fe–Al distances and partial occupation of some sites. A critical discussion of the multiple-wavelength technique is available elsewhere [Black & Corby, *Anomalous Scattering* (1975), pp. 341–359. Copenhagen: Munksgaard].


## Introduction

Measurements of diffraction intensities taken at three different wavelengths from a compound crystal can be used to calculate, for each spectrum, the intensity contribution of one of the component atoms provided the wavelengths are chosen to be in the neighbourhood of an absorption edge for that type of atom. The component atom intensities thus found may be used to obtain the structural arrangement of these atoms; this substructure, being essentially simpler than the total structure, may be determined either by Patterson methods or by sign-determining methods. It is then possible, from the calculated phases for this substructure and from the data at three wavelengths, to compute phases for all the spectra and hence to solve the complete structure. This technique has been successfully applied to the determination of the structure of $FeAl_2$ (Corby & Black, 1973) using a Patterson method to solve the Fe substructure. This paper describes the solution of the more complicated structure of α-(AlFeSi), using sign-determining methods to solve the Fe substructure, and describes and discusses the main features of the result. A more general analysis of the use of the anomalous-scattering technique in structure determination has been published (Black & Corby, 1975); this analysis is based on the results for $FeAl_2$ and α-(AlFeSi).


* Deceased.

† Present address: Centre for Science Education, Chelsea College, Bridges Place, London SW6 5HR, England.

## Theory

The intensity ${}_jI_H$ of the diffraction spectrum $H$ from a centrosymmetric structure obtained with wavelength $j$ can be written in the form

$$ {}_jI_H = A_H^2 + 2A_H\alpha_H\Delta f_j' + \alpha_H^2(\Delta f_j'^2 + \Delta f_j''^2), \quad (1) $$

where $\Delta f_j'$ and $\Delta f_j''$ represent the real and imaginary parts respectively of the wavelength dependence of the atomic-scattering factor of one type of atom in the structure, $\alpha_H$ is the geometrical structure factor for atoms of this type and $A_H$ is the amplitude for the wavelength-independent scattering for all atoms in the structure [see Corby & Black (1973) and Black & Corby (1975)]. It is assumed that the scattering factor varies with wavelength for only one type of atom. If ${}_jI_H$ is measured for three different wavelengths $j$, then the results are represented by three such equations. These will suffice to solve for $|A_H|$, $|\alpha_H|$ and a signed value for the $A_H\alpha_H$ product. The $|\alpha_H|^2$ values so obtained for each spectrum are the intensities which would have been found from a structure consisting solely of the resonant atoms. This structure is simpler than the total structure and may be solved by sign-determining methods or by Patterson methods to give signed values for $\alpha_H$. These should lead, *via* the signed $A_H\alpha_H$ product, to signed values for $A_H$ and hence directly to a complete Fourier synthesis of electron density. If this is sufficiently accurate to identify most of the atomic sites then the usual refinement techniques may be applied.

## Preliminary crystallography

There is some confusion in the literature about the numbers of phases present in the Al-rich end of the Al–Fe–Si ternary alloy system. Phillips & Varley (1943) claimed two phases, $\alpha$-(FeSi) and $\beta$-(FeSi), and subsequent disagreement involves largely the division of the $\alpha$-(FeSi) into more than one phase. Armand (1952), for instance, distinguished three phases, whilst Munson (1967) divided the area into two phases, $\alpha$ and $\gamma$.

The crystals used in the present work were a batch labelled 2·75/7·5 prepared by Pratt and described in Pratt & Raynor (1951). These same crystals have been examined by Robinson & Black (1953) who confirmed that the cell was hexagonal with $a = 12{\cdot}3 \pm 0{\cdot}1$ and $c = 26{\cdot}2 \pm 0{\cdot}2$ Å. The crystals were silvery grey metallic and the external faces showed hexagonal symmetry [see Fig. 18 of Pratt & Raynor (1951)]. Laue photographs taken with Fe radiation confirmed this and exhibited the highest Laue hexagonal symmetry $6/mmm$. Attempts to cleave the crystals failed and so a compressed-air-driven grinder as described in Bond (1951) was used to reduce them to spheres of diameter 150 $\mu$m. The spheres were mounted at random and adjusted with the aid of cylindrical Laue photographs to align the $b$ axis along the camera rotation axis.

The unit-cell dimensions at room temperature (20 °C) were calculated from measurements taken from a back-reflexion Weissenberg photograph (rotating about the $b$ axis) using unfiltered Fe radiation. The method used was an adaptation of the extrapolation method described in Buerger (1942). The wavelength standards assumed were taken from Bearden (1967): Fe $K\alpha_1$ 1·936042 Å, Fe $K\alpha_2$ 1·939980 Å, Fe $K\beta$ 1·75661 Å. The density was found to be $(3{\cdot}665 \pm 0{\cdot}004) \times 10^3$ kg m$^{-3}$ using a flotation suspension method with Clerici's solution. The weight composition was given by Pratt & Raynor (1951) as 32·53% Fe and 8·7% Si, the remainder being Al. This gave the unit-cell contents as 44·9 Fe, 167·8 Al and 23·9 Si atoms.

## Data collection

An integrating Weissenberg camera was used in the equi-inclination mode to collect three-dimensional data using filtered Fe $K\alpha$, Co $K\alpha$ and Mo $K\alpha$ radiations. A film pack containing two films only was used with the addition of an interleaving Zr foil (127 $\mu$m thickness) during the Mo $K\alpha$ exposures to increase the attenuation between films. Data were collected about the $b$ axis for layers zero to six inclusive.

A specially narrow beam trap was used during the Mo $K\alpha$ exposures to enable spectra with Bragg angles down to 1·4° to be observed; this was important because of the need to obtain as many reflexions as possible in common with the Fe $K\alpha$ and Co $K\alpha$ measurements.

The photographs were photo-electrically scanned by a drum scanner which recorded the digitized point densities on magnetic tape. The tape was subsequently analysed to give estimates of the intensities for all reflexions, subtracting in each case a local background measurement. A full description of this measurement and the analysis technique is given in the Appendix.

A few reflexions on the films were too bright to be satisfactorily measured by the drum scanner and were estimated using a double-beam microdensitometer, with a film linearity correction applied to those densities exceeding 2·0 D.

The resolution limit set by the edge effects on the Fe $K\alpha$ films was equivalent to a value of 0·50 for $\sin\theta/\lambda$. The Co $K\alpha$ intensity measurements were thus cut off at this limit. The Mo $K\alpha$ measurements, however, were continued out to a value of 0·67 for $\sin\theta/\lambda$, the extra data being introduced at a later stage in the analysis of the results. Lorentz and polarization corrections were applied.

Visual examination showed that spectra of the type ($hh2hl$, $l = 2n + 1$) were systematically absent. The (very low) values produced for these by the automatic measuring system gave a measure for the fluctuation of the system and for the lower limit of the observed reflexions.

The Mo $K\alpha$ photographs were carefully examined for any Bijvoet-pair asymmetry, but none was found within experimental error. This coupled with the above-mentioned systematic absence pointed to the centrosymmetric space group No. 194 ($P6_3/mmc$).

The crystal rotation about the $b$ axis meant that automatic inter-layer scaling was possible, *e.g.* the rows $12\bar{3}l$, $21\bar{3}l$, $\bar{1}32l$ enabled the 1st, 2nd and 3rd layers to be scaled. The many separate factors for relating the scale factors of any pair of layers were reduced by a least-squares method to six factors relating each layer to the scale of the zero layer.

The high crystal symmetry meant that a number of estimates for symmetry-related intensities existed on each film. Some reflexions, *e.g.* $12\bar{3}3$, had a total of ten estimates on the Mo $K\alpha$ films, whilst others, *e.g.* $73\bar{1}07$ on Fe $K\alpha$, had only two estimates. As a result the internal consistency in the data varied from about 3% up to 10% in intensity.

An absorption correction was made which was a function of $\theta$ only for the spherical crystals (Bond, 1959). The ratio of this correction factor between any two reflexions did not exceed a value for Fe $K\alpha$ of 3·1:1, for Co $K\alpha$ of 2·3:1 and for Mo $K\alpha$ of 1·03:1. Finally the data were put on an absolute scale by setting the average overall intensity for each wavelength to $\Sigma|f_o + \Delta f_j' + \Delta f_j''|^2$ (Wilson, 1942), where $f_o$ was evaluated for each atomic species at a weighted mean position.

## The preliminary solution

A total of 653 spectra were satisfactorily measured for each of the three wavelengths. For each spectrum the set of equations (1) was solved for $A$, $A\alpha$, and $|\alpha|^2$. The method used repeated cycles of least squares and incorporated the known functional relationship between the three variables; it is described in more detail in Black & Corby (1975).

The results showed that the $A\alpha$ product was positive in 70% of the solutions, meaning that the Fe atoms scattered in phase with the spectrum as a whole for 70% of the spectra.

The sign-determining method was applied to the $|\alpha|^2$ values assuming that they were 'spectra' for the Fe atoms alone. The actual relationship used was $S(H).S(H').S(H - H') \simeq$ positive, where the three spectra are required to be strong. The criterion of strength used initially was that the unitary structure factor ($\alpha$ divided by the number of Fe atoms per unit cell) should exceed 0·36. Eighteen satisfactory spectra were found and investigated using the above relationship. With the sign of one spectrum fixed as an origin definition, the triplet relationship yielded unambiguous signs for eight more $\alpha$ spectra. Three more were fixed with one ambiguity and the remaining six were fixed with a second ambiguity. Thus four possible sets of signs were found satisfying the triplet relationship. A Fourier synthesis of electron density was prepared for each set, Fe atoms were assigned to the peaks on each and attempts were made to define the atomic coordinates, including an occupation factor for each site. The choice between the four solutions was made by demanding that the $R$ value should be low and that the sum of the occupation factors for the Fe atoms should be close to 44, the known number of Fe atoms in each unit cell. Taken in conjunction, these criteria indicated that one of the four sets was superior to the other three and after further refinement it gave an $R$ of 23%.

Those reflexions which had both their calculated $\alpha$ from the postulated Fe structure $\geq 2{\cdot}0$ and their $\alpha$ derived from the original three wavelength data $\geq 2{\cdot}0$ were considered to be reliable in indicating signs for $A$. The Fourier electron density map formed from the 307 such reflexions was easily interpretable in terms of a satisfactory set of Fe and Al sites.

## Refinement

A least-squares full-matrix refinement (*ORFLS*, Busing, Martin & Levy, 1962) was made using all the 653 spectra. This reduced the $R$ value to about 10%. An *ad hoc* secondary-extinction correction was made using $A_{corr.} = A(1 + gA^2)$ with $g = 0{\cdot}15 \times 10^{-6}$; this had only a slight effect on the $R$ value but improved the agreement for the bright reflexions, increasing the largest $A$ by 10%.

The additional higher-resolution Mo $K\alpha$ data were then included bringing the total number of reflexions up to 1598, of which 945 were observed. The individual atomic multipliers were then allowed to be variables, where previously only a single overall scale factor had been a variable. This was done because variable occupation does seem to be common in alloy structures of this type. The refinement then showed that Al(21) at height $\frac{1}{4}$ had a significantly low occupation factor and a high temperature factor. A difference Fourier map confirmed this and suggested the presence of two more atoms, Al(22) and Al(23), close by. With these additions the structure refined eventually to $R = 5{\cdot}7\%$ with the parameters given in Table 1.*

The Si and Al atoms were assumed to be identical throughout the refinement because they have consecutive atomic numbers. A weighted least-squares comparison between the two theoretical scattering-factor curves suggests that a Si atom could be represented by an Al atom with a 102·5% occupancy

* Lists of structure factors for the measurements given for Mo $K\alpha$ wavelengths have been deposited with the British Library Lending Division as Supplementary Publication No. SUP 32738 (5 pp.). Copies may be obtained through The Executive Secretary, International Union of Crystallography, 13 White Friars, Chester CH1 1NZ, England.

Table 1. *Atomic parameters*

Each symmetrically independent atom has a reference number in parentheses. The symmetry of each atomic site is indicated with the notation of *International Tables for X-ray Crystallography* (1962). The atomic coordinates $x,y,z$ are expressed as fractions of the cell edges (multiplied by $10^4$). The occupancy multiplier has been multiplied by $10^2$ to give the percentage occupation of each site. The isotropic temperature factor $B$ is given in units of Å$^2$ ($\times 10^2$). In each case the standard error for any parameter, given in brackets following the parameter, has been given in units of the last figure, except where symmetry constraints define the parameter either uniquely or with respect to the preceding parameter. The parameters were derived from a least-squares refinement cycle based on 945 observations having an $R$ value of 5·7%.

| | Symmetry | $x$ | $y$ | $z$ | Percentage occupation | $B$ |
|---|---|---|---|---|---|---|
| Fe(1) | 12(*k*) | 5406 (1) | 812 | 1601 (1) | 99 (1) | 83 (6) |
| Fe(2) | 12(*k*) | 1305 (1) | 2610 | 1503 (1) | 100 (1) | 82 (6) |
| Fe(3) | 12(*k*) | 2160 (1) | 4320 | 9693 (1) | 103 (1) | 73 (5) |
| Fe(4) | 6(*h*) | 2084 (1) | 4168 | 2500 | 99 (2) | 64 (8) |
| Fe(5) | 4(*f*) | 3333 | 6667 | 995 (1) | 101 (2) | 85 (10) |
| Al(6) | 24(*l*) | 3467 (3) | 2906 (3) | 1027 (1) | 101 (2) | 100 (9) |
| Al(7) | 24(*l*) | 3315 (3) | 3425 (3) | 1980 (1) | 99 (2) | 78 (9) |
| Al(8) | 12(*i*) | 3726 (4) | 0 | 0 | 99 (2) | 94 (12) |
| Al(9) | 12(*k*) | 1105 (2) | 2210 | 9824 (2) | 101 (3) | 75 (11) |
| Al(10) | 12(*k*) | 4041 (2) | 8082 | 169 (2) | 101 (3) | 76 (12) |
| Al(11) | 12(*k*) | 4533 (2) | 9066 | 1063 (2) | 100 (2) | 82 (12) |
| Al(12) | 12(*k*) | 835 (2) | 1670 | 8319 (2) | 97 (3) | 76 (13) |
| Al(13) | 12(*k*) | 5968 (2) | 1976 | 814 (2) | 100 (3) | 65 (12) |
| Al(14) | 12(*k*) | 2025 (2) | 4050 | 683 (2) | 105 (3) | 118 (13) |
| Al(15) | 12(*k*) | 693 (2) | 1386 | 766 (2) | 100 (3) | 53 (12) |
| Al(16) | 12(*k*) | 2513 (2) | 5026 | 8263 (2) | 102 (3) | 124 (15) |
| Al(17) | 12(*k*) | 2521 (2) | 5042 | 1652 (2) | 100 (3) | 96 (14) |
| Al(18) | 6(*h*) | 5730 (4) | 1460 | 2500 | 96 (4) | 90 (20) |
| Al(19) | 6(*h*) | 8384 (3) | 6768 | 2500 | 100 (3) | 68 (17) |
| Al(20) | 6(*h*) | 921 (3) | 1842 | 2500 | 93 (4) | 72 (19) |
| Al(21) | 6(*h*) | 4423 (7) | 8846 | 2500 | 66 (5) | 192 (38) |
| Al(22) | 5(*h*) | 4195 (9) | 8390 | 2500 | 32 (4) | −6 (55) |
| Al(23) | 2(*c*) | 3333 | 6667 | 2500 | 29 (7) | 132 (122) |

factor and a temperature factor of −0·27 Å$^2$ additional to its intrinsic vibrational temperature factor.

Assuming a mean $B$ for Al from Table 1 of 0·86 Å$^2$ a simple equi-partition of vibrational energy argument would suggest an intrinsic $B$ for Si of 0·83 Å$^2$. Thus, any Al with a multiplier of 102·5% and a $B$ of 0·56 Å$^2$ could in reality be a Si atom. Table 1 shows Al(15), Al(19) and Al(13) as the most likely candidates but on this evidence it is not possible to identify the Si with any certainty.

## Description of the structure

Table 1 gives a list of atomic coordinates and Table 2 lists the interatomic distances. It is clear from Table 2 that the two sites Al(21) and Al(22) cannot be simultaneously occupied, nor can Al(22) and Al(23). This could have a statistical explanation in that some unit cells might have Al(21) and Al(23) simultaneously present whilst others might have Al(21) or Al(22). Suitable ratios could be chosen to give the average occupation factors of Table 1. In the Fourier synthesis of electron density of the asymmetric unit given in Fig. 1, the peak for Al(21) has been shown and those for Al(22) and Al(23) have been omitted. This simplification has been followed in all the diagrams.

Table 2 shows three significant features. Firstly, almost all of the atoms are in contact with at least eight neighbours. Secondly, no Fe atom is in contact with any other Fe atom, yet all Al atoms save Al(19) are in contact with at least one Fe atom. Thirdly, the smallest Fe–Al distances involve Al atoms which are themselves bound to the smallest number of Fe atoms; Al(9) has only one Fe neighbour [Fe(3)] and the interatomic separation is the smallest in the structure at 2·29 Å. Similarly Al(15) having only one neighbour [Fe(2)] shows the next smallest separation of 2·34 Å. The overall mean Fe–Al distance for those with two Fe neighbours is 2·47 Å whilst for those with three it is 2·59 Å. Similar features have been observed in other Fe–Al structures (see Black, 1956).

Although it may not be obvious in Fig. 1, a hole has been found at the origin of the unit cell. The distances of this hole to its neighbours are shown in Table 2. The presence of only six Al neighbours, Al(9), means that the site is unlikely to be occupied by Fe, whilst the separation of 2·42 Å is too small to enable the site to be occupied by Al.

As no Fe atom is in contact with any other Fe atom, the structure can be described in terms of Al linkages between Fe-centred polyhedra (see Black, 1956). The five such polyhedra are shown in Fig. 2 with a projection and orientation consistent with that of Fig. 1.

Table 2. *Individual and mean interatomic distances*

The distances are given in Å from each atom of the asymmetric unit to all atoms within a 3·0 Å sphere; accuracies are expected to be within ±0·01 Å. The identity of the neighbouring atom is given in round brackets, followed where necessary by a post multiplier indicating the number of symmetry-related neighbours each at the same distance. The last two columns give the mean Fe–Al and Al–Al interatomic distances for each atom considered to be in contact with its neighbour. The total number of each type of neighbour in contact is appended in curly brackets.

| | Symmetry | Fe neighbours | Al neighbours | Mean Fe–Al distance | Mean Al–Al distance |
|---|---|---|---|---|---|
| Fe(1) | 12(*k*) | | 2·72 (6) × 2, 2·45 (7) × 2, 2·35 (11), 2·40 (13), 2·41 (16) × 2, 2·46 (18) | 2·49 {9} | |
| Fe(2) | 12(*k*) | | 2·81 (6) × 2, 2·51 (7) × 2, 2·50 (12) × 2, 2·64 (14), 2·34 (15), 2·65 (17), 2·75 (20) | 2·60 {10} | |
| Fe(3) | 12(*k*) | | 2·55 (6) × 2, 2·53 (8) × 2, 2·29 (9), 2·54 (10) × 2, 2·57 (13) × 2, 2·62 (14) | 2·53 {10} | |
| Fe(4) | 6(*h*) | | 2·54 (7) × 4, 2·41 (17) × 2, 2·51 (20), 2·54 (21) × 2, 2·38 (22) × 2, 2·69 (23) | 2·50 {12} | |
| Fe(5) | 4(*f*) | | 2·64 (10) × 3, 2·58 (11) × 3, 2·93 (14) × 3, 2·45 (17) × 3 | 2·55 {9} | |
| Al(6) | 24(*l*) | 2·72 (1), 2·81 (2), 2·55 (3) | 2·89 (6), 2·61 (7), 2·85 (8), 2·99 (9), 2·77 (11), 2·96 (12), 2·76 (13), 2·93 (14), 2·89 (16) | 2·69 {3} | 2·84 {9} |
| Al(7) | 24(*l*) | 2·45 (1), 2·51 (2), 2·54 (4) | 2·61 (6), 2·73 (7), 2·94 (12), 2·93 (16), 2·77 (17), 2·96 (18), 2·59 (19), 2·97 (20), 2·68 (21), 2·94 (22) | 2·50 {3} | 2·81 {10} |
| Al(8) | 12(*i*) | 2·53 (3) × 2 | 2·85 (6) × 2, 2·86 (9) × 2, 2·65 (10) × 2, 2·95 (14) × 2 | 2·53 {2} | 2·85 {8} |
| Al(9) | 12(*k*) | 2·29 (3) | 2·99 (6) × 2, 2·86 (8) × 2, 3·00 (14), 2·59 (15) × 2 | 2·29 {1} | 2·84 {8} |
| Al(10) | 12(*k*) | 2·54 (3) × 2, 2·64 (5) | 2·65 (8) × 2, 2·61 (10) × 2, 2·55 (11), 2·59 (13), 2·78 (14) × 2 | 2·57 {3} | 2·65 {8} |
| Al(11) | 12(*k*) | 2·35 (1), 2·58 (5) | 2·77 (6) × 2, 2·55 (10), 2·87 (14) × 2, 2·77 (17) × 2 | 2·47 {2} | 2·77 {7} |
| Al(12) | 12(*k*) | 2·50 (2) × 2 | 2·96 (6) × 2, 2·94 (7) × 2, 2·91 (15) × 2, 2·74 (19), 2·86 (20) × 2 | 2·50 {2} | 2·90 {9} |
| Al(13) | 12(*k*) | 2·40 (1), 2·57 (3) × 2 | 2·76 (6) × 2, 2·59 (10), 2·58 (13) × 2, 2·92 (16) × 2 | 2·52 {3} | 2·73 {7} |
| Al(14) | 12(*k*) | 2·64 (2), 2·62 (3), 2·93 (5) | 2·93 (6) × 2, 2·95 (8) × 2, 3·00 (9), 2·78 (10) × 2, 2·87 (11) × 2, 2·87 (15), 2·75 (17) | 2·63 {2} | 2·88 {11} |
| Al(15) | 12(*k*) | 2·34 (2) | 2·62 (9), 2·59 (9) × 2, 2·91 (12) × 2, 2·87 (14), 2·57 (15) × 2 | 2·34 {1} | 2·70 {8} |
| Al(16) | 12(*k*) | 2·41 (1) × 2 | 2·89 (6) × 2, 2·93 (7) × 2, 2·92 (13) × 2, 2·76 (18) × 2, 2·78 (19) | 2·41 {2} | 2·86 {9} |
| Al(17) | 12(*k*) | 2·65 (2), 2·41 (4), 2·45 (5) | 2·77 (7) × 2, 2·77 (11) × 2, 2·75 (14), 2·84 (22) × 2, 2·82 (23) | 2·50 {3} | 2·79 {8} |
| Al(18) | 6(*h*) | 2·46 (1) × 2 | 2·96 (7) × 4, 2·76 (16) × 4, 2·81 (21) | 2·46 {2} | 2·83 {9} |
| Al(19) | 6(*h*) | | 2·59 (7) × 4, 2·74 (12) × 2, 2·78 (16) × 2 | | 2·67 {8} |
| Al(20) | 6(*h*) | 2·75 (2) × 2, 2·51 (4) | 2·97 (7) × 4, 2·86 (12) × 4 | 2·67 {3} | 2·92 {8} |
| Al(21) | 6(*h*) | 2·54 (4) × 2 | 2·68 (7) × 4, 2·81 (18), 0·54 (22), 2·34 (23) | 2·54 {2} | 2·70 {5} |
| Al(22) | 6(*h*) | 2·38 (4) × 2 | 2·94 (7) × 4, 2·84 (17) × 4, 0·54 (21), 1·81 (23) | 2·38 {2} | 2·89 {8} |
| Al(23) | 2(*c*) | 2·69 (4) × 3 | 2·82 (17) × 6, 2·34 (21) × 3, 1·81 (22) × 3 | 2·69 {3} | 2·82 {6} |
| Origin hole | | | 2·42 (9) × 6 | | |

Those Al atoms masked by others are shown with an arrow indicating their position.

The polyhedra centred on Fe(1) and Fe(2) are together shown in Fig. 3. The Al(16) atoms provide the self linkages between the Fe(1) polyhedra; the Al(12) atoms play a similar role for Fe(2) whilst Al(6) and Al(7) link the two types of polyhedra into one continuous sheet (type *A* sheet). Al(18) and Al(20) at height $\frac{1}{4}$ lie on this polyhedral sheet and link it to its mirror image *A'* (the mirror being at height $\frac{1}{4}$).

The polyhedra centred on Fe(3) are shown in Fig. 4 with Al(8), at height zero, and Al(10) and Al(13) providing the self linkages which form the continuous puckered sheet (type *B* sheet). The sheet contains the unit-cell origin and thus exhibits centrosymmetry unlike the type *A* sheet.

The two types of sheet are linked by their common atoms Al(6), Al(13) and Al(14). The remaining Fe atoms serve to reinforce the joining of the sheets with Fe(4), lying in the mirror at height $\frac{1}{4}$, joining *A* to *A'* whilst Fe(5) joins *A* to *B*. The sheets finally stack in three dimensions as *A'BA*(*M*)*A'B'A*, where (*M*) indicates the height $\frac{1}{4}$ mirror plane.

## Conclusions

The main features of this structure are consistent with features shown by $Fe_2Al_5$ (Forsyth, 1959), $Fe_4Al_{13}$ (Black, 1955) and $Fe(Cu,Al)_6$ (Black, Edwards & Forsyth, 1961). It is possible to represent the composition of α-(FeAlSi) as $Fe(Si,Al)_{4\cdot2}$ or as $FeAl_{3\cdot7}Si_{0\cdot5}$

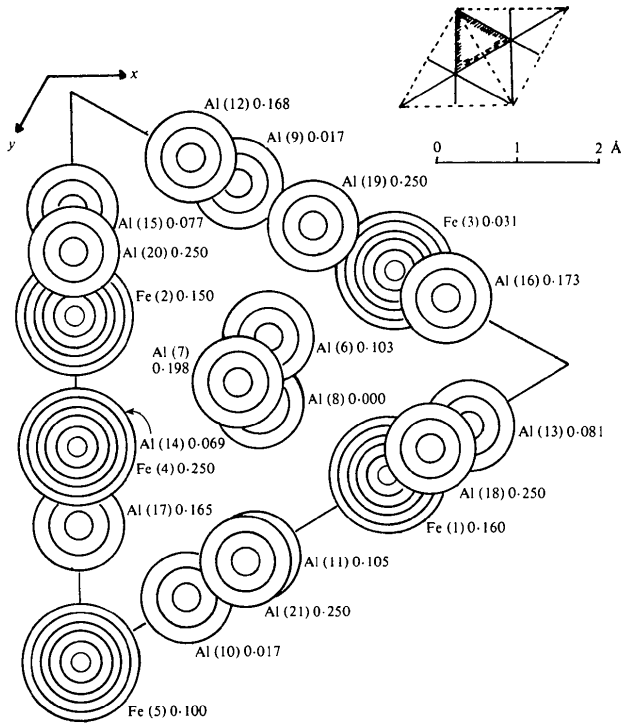


Fig. 1. The top right of the figure shows the unit cell viewed along the hexagonal axis; dotted lines are projections of glide planes, whilst the solid lines are projections of mirror planes. The asymmetric unit, considered to extend from $z = 0$ to $z = \frac{1}{4}$, is shown with a shaded border. The figure indicates the contents of the asymmetric unit by sections of the three-dimensional electron density synthesis taken through the centre of each atom. The contours are drawn at arbitrary intervals. The identity of each atom is followed by its $z$ coordinate. Note that Al(11) is partially masked by Al(21), and that Al(14) is completely masked by Fe(4).

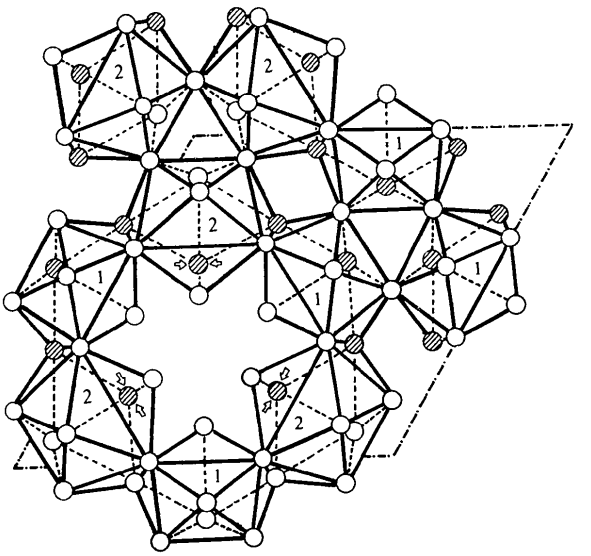

Fig. 3. The type *A* sheet formed from Fe(1)- and Fe(2)-centred polyhedra; the numbers identify the polyhedra. The picture has been extended beyond the unit-cell boundaries, indicated by a line of alternating dots and dashes, to show the disposition round the (0,0), $(\frac{1}{3},\frac{2}{3})$ and $(\frac{2}{3},\frac{1}{3})$ sites. The mean height of this sheet is 3·86 Å above the basal plane. The mirror plane at height $\frac{1}{4}$ (6·56 Å above the basal plane) contains the Fe(4) atoms [with positions shown by pairs of arrows, the $x,y$ coordinates are almost the same as for Al(14)] which serve to join the sheet to its mirror image *A'* at 9·26 Å above the basal plane. The apparent hole at $(\frac{1}{3},\frac{2}{3})$ is occupied by Fe(5) which serves to bind this sheet to the type *B* sheet below. Shaded atoms are those Al(6), Al(13) and Al(14) atoms which are common to the type *B* sheet of Fig. 4.

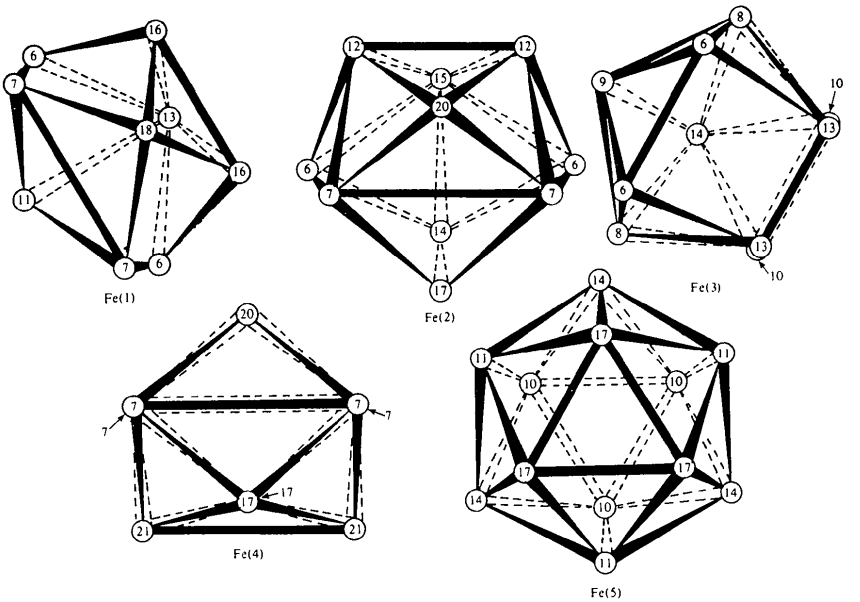


Fig. 2. The Fe-centred Al polyhedra. The immediate environment of each of the five Fe atoms is shown in an orientation consistent with that of Fig. 1. The lines connecting the Al atoms serve to aid in visualizing the polyhedra and do not necessarily represent bonds or atoms in contact.

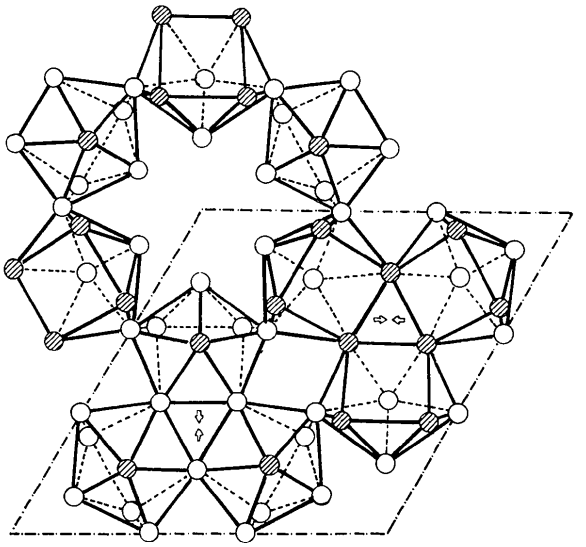

Fig. 4. The type *B* sheet formed from Fe(3)-centred polyhedra. The picture is extended in the same way as in Fig. 3 and shows the hole at (0,0). The mean level of this sheet is in the basal plane. The Fe(5) atom at 2·63 Å above the basal plane (position shown by the vertical pair of arrows) serves to bind this sheet to the type *A* sheet above. The Fe(5) atom at 2·63 Å below the basal plane (position shown by the horizontal pair of arrows) serves to bind the sheet to the *A'* sheet below. The perspective is such that all Al(10) atoms are concealed (see Fig. 2). Shaded atoms are those Al(6), Al(13) and Al(14) atoms which are common to the type *A* sheet of Fig. 3.

but because of the difficulty of distinguishing Al from Si it is not possible to speculate about the possible role of Si in the structure. $Fe(Cu,Al)_6$ is an Fe–Al compound, richer in Al than any in the binary system, which is 'stabilized' by a small amount of a third element which plays no obvious role in the crystal structure; it may be significant that α-(FeSiAl) has similar properties.

This work shows the power of the multiple-wavelength technique and illustrates that it may be regarded as extending the range of any technique which is sufficiently powerful to solve the resonant-atom substructure. A more detailed discussion of the possibilities of the technique has been given elsewhere (Black & Corby, 1975).

We thank the Science Research Council for support of this work and the Laboratory for Molecular Biophysics, Department of Zoology, University of Oxford, for the use of their Optronics optical scanner. We are also grateful to several colleagues, particularly Professor A. J. C. Wilson, for helpful discussions and for support for and interest in this work.

## APPENDIX
### The intensity-measuring system

An automatic method was needed to measure the full set of three-dimensional data from a crystal with a large unit cell at three wavelengths. The method had to be capable of accurate location because the distance between adjacent reflexions, particularly on integrated photographs taken with Mo $K\alpha$, was so small that the risk of mis-indexing was appreciable. These two requirements were met by using an Optronics automatic drum scanner. This machine enabled the optical density of all points on the film to be written on a magnetic tape. A computer program extracted the individual densities of all reflexions from this magnetic tape.

Each film was mounted on the hollow drum of the scanner, the rotation of which caused a narrow strip of film to intercept and attenuate a fine light beam. The intensity of the resultant beam was measured by a photo-electric cell and expressed as an integer on a scale from 0 to 255 (the maximum being equivalent to 2·0 D, which was approximately the linearity limit for the film in use). Densities were recorded for points separated by 100 μm along each strip, and were written as a block to the magnetic tape. The drum was then moved 100 μm along its axis and the process repeated. Thus the optical density of the whole film was sampled at points over an orthogonal grid of cell side 100 μm. Typically 10 min were taken to scan a film area of 7 × 15 cm. Prior to transferring each data block to the tape a monotonically increasing integer (known as the block number) was written to the tape. This integer corresponded to the $x$ coordinate, $x$(tape), of the strip, whereas the $y$ coordinate, $y$(tape), of each density point was represented by its position within its data block.

The ideal coordinates $x$(ideal) and $y$(ideal) of all possible reflexions can be computed for each Weissenberg photograph and are a known function of the unit cell, the crystallographic rotation axis, the wavelength, the camera-cassette radius and the angular limits of the crystal's oscillation. Throughout this experiment the crystal was rotated about the $b$ axis so that the intersection of the $c^*$ axis with the rotation axis is a natural origin for the ideal coordinate frame.

A small hole was drilled in each film prior to the drum-scanner measurement at the point corresponding to the above origin. Its location in the tape-coordinate frame was found by a program which scanned the magnetic tape and reported the mean position of points of zero density (the hole by definition has zero density). The same program gave the tape coordinates, referred to the hole as origin, of those dark areas on the film whose density exceeded a specified threshold ($T$). These when plotted on graph paper could be easily compared with the original film and with the lists of ideal coordinates, enabling light leaks and dust specks to be rejected. The value of $T$ was so chosen that

twenty or so reflexions were selected in this way. They were chosen to be well spread over the film, and for each the tape and the ideal coordinates were noted. These were given to a second program which computed by a least-squares method six parameters defining a linear relationship connecting the two frames. The parameters can be interpreted as a simple $x$–$y$ shift, a rotation equivalent to film skew in the camera or the drum scanner, a radius error due to the finite thickness of the multiple film pack, and a film-shrinkage error. Two additional parameters were defined corresponding to crystal-alignment errors. The ideal coordinates of all possible reflexions could now be computed and transformed by the above parameters to tape-coordinate form.

As the films were integrated Weissenbergs, only the plateau density at the centre of each spot was required to provide an estimate of the integrated intensity of the reflexion. To estimate the local background four neighbouring positions were taken surrounding each reflexion. White radiation tails were seen from many of the stronger reflexions on Mo $K\alpha$ photographs. These could easily have led to heavy overestimation of any reflexions that lay in their paths. To provide a warning of such a presence a fifth background position was measured for each reflexion, at a neighbouring site chosen to be in the direction of the origin of reciprocal space. The $K\beta$ filter guarantees that this position is locally 'clean' as far as the reflexion's own tail is concerned. It will be appreciated that the direction referred to cannot in general be exact on other than zero-layer photographs; in the event it proved sufficient. If there was no significant 'tail problem' the value of this fifth background would not differ significantly from the mean of the other four. Thus a total of six specific sites were defined for each reflexion. For each site four, five or six grid points were selected close to the computed tape coordinates. Thus a grand total of between 24 and 36 point densities were needed for the measurement of each reflexion.

The integer coordinates and some system information were compacted into a single-integer computer word, and the crystallographic index was similarly compacted into a single half-length computer word. These sets of integer coordinates were then put into the order in which they would occur on the data tape, that is in order of block numbers (not a detailed dictionary order), the ordering instructions being recorded on a scratch magnetic tape. The actual measurement was simply a single pass through the data tape reading a block at a time, extracting from it those point densities wanted and overwriting the now unwanted coordinates with the point densities themselves. The scratch tape was then read 'backwards' to extract the re-ordering instructions required to recover the original *hkl* order in the computer core.

Finally a print-out of each intensity minus background was made, together with comments on any difficult features. Examples of such features were: an excessive spread of the individual density points defining a site, an excessive spread of individual means of the four background sites or a white-tail background site excessively different from the other four background sites. About 15% of the reflexions gave difficulty, and for these a detailed listing was made of all the intensity data points. From these lists the difficulty was often easily resolved and suitable adjustments made to the final intensity-minus-background figure. A very few reflexions, less than 1%, had to be rejected from the lists completely.

## References


ARMAND, M. (1952). *C. R. Acad. Sci. Paris*, **235**, 1506–1508.

BEARDEN, J. A. (1967). *Rev. Mod. Phys.* **39**, 78–124.

BLACK, P. J. (1955). *Acta Cryst.* **8**, 175–182.

BLACK, P. J. (1956). *Acta Metall.* **4**, 172–179.

BLACK, P. J. & CORBY, R. N. (1975). *Anomalous Scattering*, pp. 341–359. Copenhagen: Munksgaard.

BLACK, P. J., EDWARDS, O. S. & FORSYTH, J. B. (1961). *Acta Cryst.* **14**, 993–998.

BOND, W. L. (1951). *Rev. Sci. Instrum.* **22**. 344.

BOND, W. L. (1959). *Acta Cryst.* **12**, 375–381.

BUERGER, M. J. (1942). *X-ray Crystallography*, pp. 435–465. New York: John Wiley.

BUSING, W. R., MARTIN, K. O. & LEVY, H. A. (1962). *ORFLS*. Report ORNL-TM-305. Oak Ridge National Laboratory, Tennessee.

CORBY, R. N. & BLACK, P. J. (1973). *Acta Cryst.* B**29**, 2669–2677.

FORSYTH, J. B. (1959). PhD Thesis, Univ. of Cambridge, England.

*International Tables for X-ray Crystallography* (1962). Vol. III. Birmingham: Kynoch Press.

MUNSON, D. (1967). *J. Inst. Met.* **95**. 217–219.

PHILLIPS, H. W. L. & VARLEY, P. C. (1943). *J. Inst. Met.* **69**, 317–350.

PRATT, J. N. & RAYNOR, G. V. (1951). *J. Inst. Met.* **79**, 211–232.

ROBINSON, K. & BLACK, P. J. (1953). *Phil. Mag.* **44**, 1392–1397.

WILSON, A. J. C. (1942). *Nature, Lond.* **150**, 151–152.